Hindawi
Journal of Nanotechnology
Volume 2023, Article ID 9572025, 9 pages
https://doi.org/10.1155/2023/9572025

Research Article

Synthesis of Green Cerium Oxide Nanoparticles Using Plant Waste from *Colocasia esculenta* for Seed Germination of Mung Bean (*Vigna radiata*)

Nor Monica Ahmad[1,2] **and Nor' Aishah Hasan**[2,3]

[1]*School of Chemistry and Environment, Faculty of Applied Sciences, Universiti Teknologi MARA, Cawangan Negeri Sembilan, Kampus Kuala Pilah, Kuala Pilah 72000, Malaysia*
[2]*Biotechnology, Microbiology and Environment Collaborative Sciences, Universiti Teknologi MARA (UiTM), Cawangan Negeri Sembilan, Kampus Kuala Pilah, Kuala Pilah 72000, Negeri Sembilan, Malaysia*
[3]*School of Biology, Faculty of Applied Sciences, Universiti Teknologi MARA, Cawangan Negeri Sembilan, Kampus Kuala Pilah, Kuala Pilah 72000, Malaysia*

Correspondence should be addressed to Nor Monica Ahmad; normonica@gmail.com

Received 28 June 2022; Revised 28 November 2022; Accepted 2 April 2023; Published 30 May 2023

Academic Editor: Carlos Cabrera

Synthesis of cerium oxide (CeO_2) nanoparticles (NPs) via biological approach has received a lot of interest to reduce the harmful effects of chemical synthesis. In the present study, *Colocasia esculenta* leaf extract facilitated the preparation of CeO_2-NPs by using the sol-gel technique. The crystal structural of CeO_2-NPs was proven by X-ray powder diffraction (XRD) investigation to be cubic with size of 2.94 nm according to Debye–Scherrer equation. As demonstrated in the transmission electron microscopy (TEM) image, CeO_2-NPs have a spherical form with an average size of 2.04 nm which is almost consistent with a finding from XRD analysis. Energy dispersive X-ray (EDX) measurements exhibited high-intensity peaks attributed to Ce and oxygen and further proved the creation of CeO_2-NPs. The Fourier transform infrared spectroscopy (FTIR) analysis revealed the presence of Ce-O stretching, indicating the formation of CeO_2-NPs. Functional groups of O-H, C-O, and C=O peaks were found in a spectrum due to the phytochemical components that were responsible for reducing and stabilizing during the synthesis process of CeO_2-NPs. The examined UV-visible spectra exhibited the absorbance peak at 213 nm. The synthesized NPs produced in this study were further investigated for mung bean seed germination, whereby the influence of grain germination and growth rate demonstrated the significant finding.

1. Introduction

Nanoparticles (NPs) are defined as an atom having a diameter range of 1 nm–100 nm [1]. A variety of NPs were fabricated in the past few years such as titanium oxide NPs [2], silver NPs [3], silica NPs [4], iron oxide NPs [5], and copper NPs [6]. Among them, cerium oxide NPs (CeO_2-NPs) owing to their excellent electronic, eco-friendly properties, and tremendously growing catalytic applications, have exhibited tremendous contribution diversity of applications such as therapeutic agent [7], antibacterial agent [8], for impaired diabetic wound healing [9], agent for anticancer [10], and fuel cell [11]. Among these fields, attention should be given to an agriculture field as they play an important role for fiscal economy to many countries, however suffer from the insufficient production of market supply to meet a growing demand of crops plants worldwide. As a solution, fertilizers have been introduced to crop plants to boost the crop production. However, the usage of excess fertilizer to plants creates a future problem to the ecology and environment. Therefore, scientists recommended reducing the quantity of fertilizer to plant and soil to secure sustainability of nature. The efforts are made

possible by using nanofertilizers such as zinc oxide NPs [12, 13], copper NPs [14], and iron oxide NPs [15]. To date, NPs display a promising platform to boost plant growth of cabbage [16], maize [17], mung bean [18], and rice [19]. Despite the advantages of the nanosize of cerium oxide, their investigation as nanofertilizer is still limited.

The common approach to synthesis CeO_2-NPs are through physical and chemical approaches. However, it has been observed that the aforementioned approaches for the synthesis of CeO_2-NPs had several limitations, including the use of toxic chemicals and high-tech automation and incur high cost of chemicals. Of these, biological approach offers a "green" synthesis method with inexpensive method by using abundant natural biological species such as fungus [17], bacteria [20], plants [14], and algae [21]. They act as a reducing agent, stabilizer, and capping agent in the synthesis route which have the potential to substitute expensive chemical capping agents. Previous study had utilized triethanolamine (TEA), ethylene diamine tetra acetic acid (EDTA), tetraethylammonium bromide (TEABr) [22], ethylenediamine (EDA), hexamethylediamine (HTMA) [23], 1-dodecyl-3-methylimidazolium bromide [24], tri-n-octyl phosphine oxide (TOPO), and dodecyle amine (DDA) [25] due to their available bulky and steric hindrance structures. The traditional sol-gel procedures are commonly used to synthesis NPs, but they have various drawbacks, including self-aggregation, uneven distribution of particle size and shape, and nanocluster formation. By using an appropriate capping agent throughout the synthesis phases, agglomeration effects and other limitations of the sol-gel method can be easily overcome [26].

The "green" synthesis of NPs had gain attention in the past two decades to secure environment and achieve sustainability. The leaves waste from *Colocasia esculenta* (*C. esculenta*), commonly known as Taro, generate a biowaste from leaves which are plentifully obtainable in Malaysia without any profitable application. As compared to other root crops, *C. esculenta* produces highly nutritious leaves (petiole and blades), which are high in carbohydrates, proteins, minerals, vitamins, and other phytonutrients with antioxidant potential [27]. These advantages allow them to act as reducing and stabilizing agents in the synthesis of CeO_2-NPs. The plant has been reported as reducing and stabilizing agents in the earlier work by Inamuddin and Kanchi [28]. In their work, *C. esculenta* had successfully impacted on the synthesis of silver NPs indicating the great potential for biological approach in NPs synthesis [28]. To the best of author's knowledge, no research had been published previously on the potential of their leaves extract to stabilize the "green" synthesis of CeO_2-NPs. Regardless of the fact that the plants are rich in nutrient [29], one of the earliest domesticated plants [27] and substantially adaptable, Taro is still regarded as an orphan crop. Therefore, the present study will synthesize CeO_2-NPs by using leaves extract from *C. esculenta* for mung bean (*Vigna radiata*) seed germination. The morphology, structural, size, and optical properties of synthesized CeO_2-NPs were investigated in detail.

2. Experimental

2.1. Chemicals and Reagents. Cerium (III) nitrate hexahydrate [$Ce(NO_3)_3 \cdot 6H_2O$] was purchased from Sigma-Aldrich Corporation (United States). Analytical grade of ethanol was from Chemiz (M) Sdn. Bhd. (Malaysia). The chemicals were used without further purifications. The deionized water was used throughout the experiment during synthesis and germinations.

2.2. Preparation of C. esculenta Leaf Extract. Leaves from *C. esculenta* were collected from Malaysian Agricultural Research and Development Institute (MARDI), Selangor, and thoroughly washed, dried under shed, and finely ground to obtain homogeneous and fine powder. The powder was kept sealed in a plastic petri dish until further use. Then, 10 g powdered leaves were heated in 100 mL of deionized water for 15 min at 80°C and then incubated at room temperature overnight. The resulting solution was filtered by using a cotton cloth to remove any residue. The filtrate was used for the synthesis of CeO_2-NPs.

2.3. Synthesis of CeO_2-NPs. The synthesis of CeO_2-NPs followed a method by Mathew et al. [18] with a slight modification. *C. esculenta* leaf extract of 100 mL was mixed with 0.11 M of $Ce(NO_3)_3 \cdot 6H_2O$ to prepare a solution. The solution was constantly stirred with a magnetic stirrer at 80°C for 4 h. The resulting solution was centrifuged. Water and ethanol were added few times during centrifuge. The collected CeO_2-NPs was poured onto a glass plate, oven dried at 60°C overnight, and calcined at 400°C for 3 h. The obtained yellow powder NPs were ground and kept in a seal bottle prior to characterization. The schematic representation of CeO_2-NPs synthesis through *C. esculenta* leaf extract is demonstrated in Figure 1.

2.4. Characterizations of CeO_2-NPs. The synthesized NPs were characterized by using T80+ UV/Vis spectrophotometer (PG Instruments) between 200 nm and 600 nm. In X-rays, powder diffraction (PAN analytical X-ray diffractometer operated at 45 kV and Rayon X on 40 mA (Cu-Kα radiation 1.5 Å)) in the 2θ range from 20° to 80° was used to evaluate their crystalline nature and particle sizes. Field emission scanning electron microscopy (FESEM) with EDX-analysis (MERLIN Compact) and transmission electron microscopes (Talos L120C) were performed for surface morphology and shape. The structural changes of CeO_2-NPs were determined by using Fourier transform infrared spectroscopy (FTIR) (Perkin Elmer) in the 4000 cm^{-1}–400 cm^{-1} range.

2.5. Germination Assay. Seed germination assay followed a method by Mathew et al. [18] with a slight modification. In brief, mung bean (*Vigna radiata*) seeds were placed in a beaker containing distilled water for 2 min-3 min for cleansing purpose and left to dry on papers for 10 min at room temperature. Later, 15 seeds of similar size were

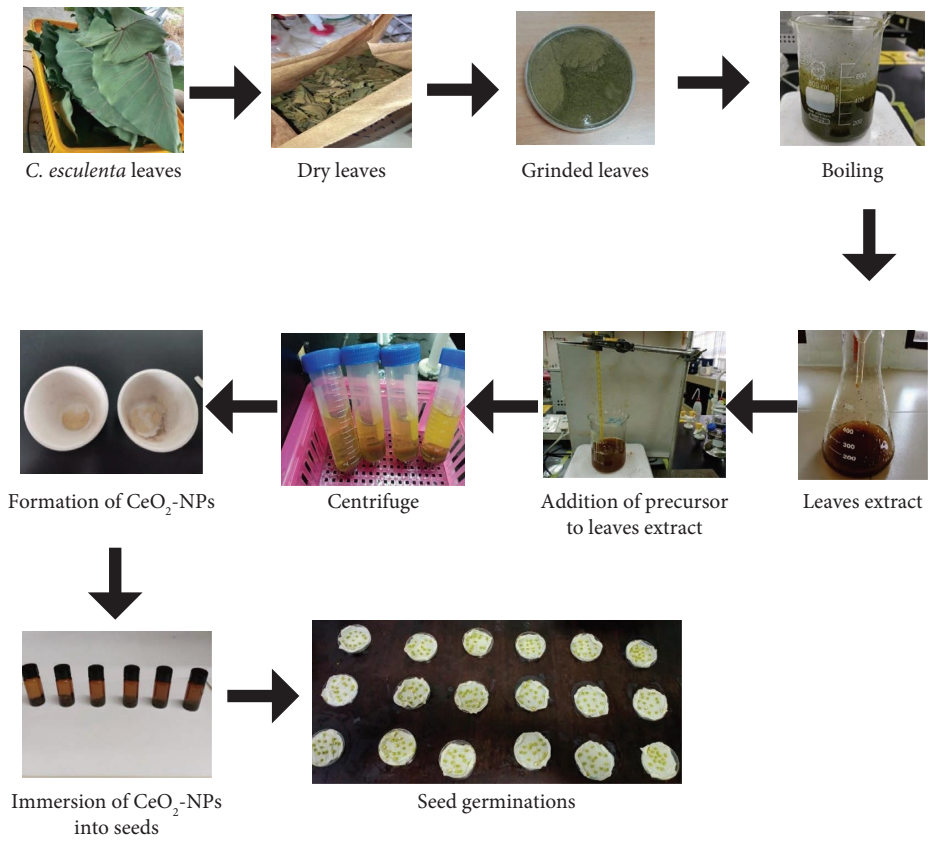

Figure 1: Synthesis process of CeO_2-NPs and application to mung bean.

selected and immersed in amber bottles that contained different concentrations of CeO_2-NPs for 2 h. A control was made by placing 15 seeds inside the amber bottle that contained only distilled water. The serial dilution of required concentration was prepared according to Awan et al. [30]. The stock concentrations of CeO_2-NPs were made by using 50 mg in 1 mL of deionized water. Then, a dilution to 0.5 mg·mL^{-1}, 1.0 mg·mL^{-1}, 1.5 mg·mL^{-1}, 2.0 mg·mL^{-1}, and 2.5 mg·mL^{-1} was conducted by using 10 mL of deionized water to immerse seeds of Vigna radiata. The seeds were spread on moistened cotton surfaces at a rate of 15 seeds per plate. Seed germination was observed daily for 7 days after the germination test was started. Data obtained from the inhibition zone were analysed by using analysis of variance (ANOVA). Tukey's test was performed to compare the mean differences among treatment at probability level of 0.05 by using SPSS Statistics version 23.

3. Results and Discussions

3.1. Synthesis and Characterization of CeO_2-NPs. The formation of CeO_2-NPs was indicated by the formation of a thicker solution after 0.11 M of $Ce(NO_3)_3 \cdot 6H_2O$ solution was added to 100 mL of *C. esculenta* leaf extract, stirred for 4 h at 80°C, and revealed the gradual reduction of Ce^{4+} to Ce^0. According to Utara et al. [31] and Calvache-Muñoz et al. [32], the mechanism for the formation of CeO_2-NPs is shown as follows:

$$\begin{aligned}
&Ce(NO_3)_3 \cdot 6H_2O \longrightarrow Ce^{3+} + 3NO_3^- + 6H_2O,\\
&Ce^{3+} + H_2O \longrightarrow Ce(OH)^{3+} + H^+ + e^-,\\
&Ce^{4+} + 4OH^- + xH_2O \longrightarrow Ce(OH)_4 \cdot xH_2O,\\
&Ce(OH)_4 \cdot xH2O \longrightarrow Ce(OH)_4 + xH_2O,\\
&Ce(OH)_4 \longrightarrow CeO_2 + 2H_2O.
\end{aligned} \tag{1}$$

When dissolved in plant extract, the precursor dissociated into Ce^{3+}, $3NO^-_3$, and $6H_2O$. Further reaction would produce $Ce(OH)^{3+}$ as in Step 2. In Step 3, Ce that had oxidation number of +4 from $Ce(OH)^{3+}$ reacted with hydroxide and water to form $Ce(OH)_4{\cdot}xH_2O$. Heating process at Step 4 would produce $Ce(OH)_4$ as the process would remove water from the molecule. Calcination was carried out to completely remove hydroxide from $Ce(OH)_4$ to produce CeO_2-NPs.

3.2. UV-Vis Spectroscopy. UV-vis spectroscopy was utilized to examine the formation of CeO_2-NPs from the plant extract at 200 nm–600 nm wavelength as displayed in Figure 2. The spectrum exhibited an absorbance peak at 213 nm indicating the development of CeO_2-NPs. Based on a previous study, common absorbance peak of CeO_2-NPs was found at 332 nm when citrate-nitrate sol-gel method was utilised [33]. Another possible absorption peak was found at 284 nm when CeO_2-NPs were synthesized by using hexamethylenetetramine as demonstrated by Parimi et al. [34].

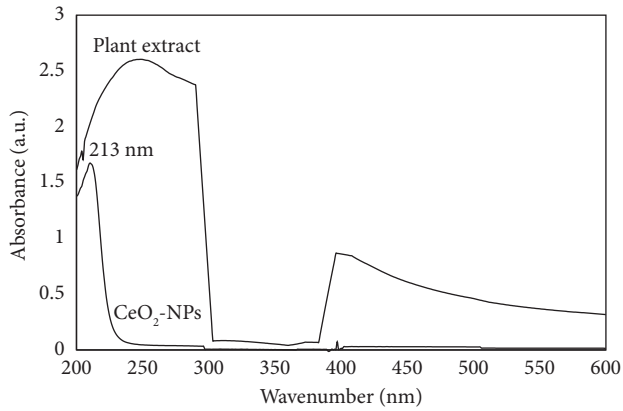

Figure 2: UV–visible absorption spectrum of CeO_2-NPs.

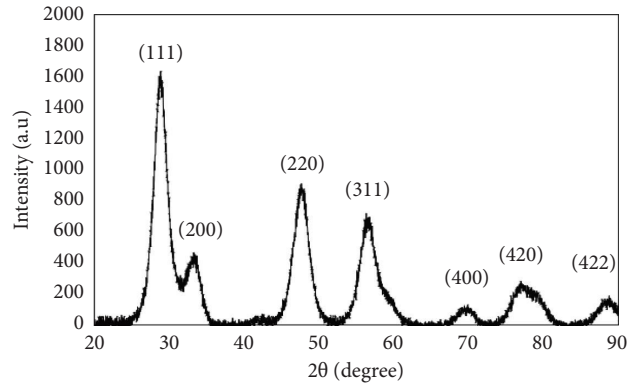

Figure 3: X-ray diffraction spectra of CeO_2 nanoparticles.

Likewise, Arumugam et al. synthesized CeO_2-NPs using Gloriosa superba L. leaf extract, and the NPs exhibited the absorption peak at 297 nm [35]. In the present study, the absorption band occurs at a lower wavelength known as blue shift phenomenon. This was due to the small size of CeO_2-NPs that causes this effect as experienced by Krishnamoorthy et al. [36]. In addition to the absorbance, the formation of CeO_2-NPs was confirmed visually through the yellowish powder of final NPs after furnace. Eka Putri et al. [37] synthesized CeO_2-NPs by using Moringa oleifera leaf extract as a natural bio-reducing agent to reduce a precursor to produce CeO_2-NPs. According to their study, the color change was a visible production indicator of CeO_2-NPs. As a result, the role of leaf extract as a reducing agent had been confirmed. Another function of Taro's plant extract serves as a capping agent, whereby it also assists to keep nanoparticles growing and manage their size; hence, it serves as a stabilizer [37].

3.3. XRD Analysis. The X-ray diffraction technique was used to determine the crystalline structure and size of CeO_2-NPs. Figure 3 shows the finer and more persistent diffraction peaks demonstrated the crystallinity of CeO_2-NPs. CeO_2-NPs did not contain any contaminants, as evidenced by the absence of any other diffraction peaks from other species. The X-ray diffraction spectra presented characteristic diffraction peaks at 11.77°C, 28.89°C, 33.68°C, 48.14°C, 57.16°C, 71.07°C, 77.27°C, and 88.37°C. The crystal size of CeO_2-NPs, calculated by using Debye–Scherrer equation, was found to be 2.94 nm.

$$D = k\lambda, \quad \beta \cos \theta, \tag{2}$$

where k is the Scherrer constant having a value 0.94, λ is the wavelength of X- ray, β is half-width at half- maximum (FWHM) data with intensity and position is provided by XRD patterns, θ is the Bragg diffraction angle, and D is the particle size [38]. The XRD diffraction patterns of CeO_2-NPs were found in accordance with the finding from Ahmad et al. [39], whereby Elaeis guineensis leaves were used as a reducing and stabilizing agent in the formation of CeO_2-NPs [39]. In addition, another study by Iqbal et al. [40] utilized Phoenix dactylifera plant extract demonstrated similar XRD diffraction pattern of CeO_2-NPs [40].

3.4. FESEM-EDX Analysis. FESEM analysis evaluated morphological image of CeO_2-NPs synthesized in leaf extract, crystallography, and evaluation of gradient chemical composition of the NPs [41]. Figure 4 shows a FESEM image of CeO_2-NPs produced from *C. esculenta* leaf extract. As demonstrated in Figures 4(a) and 4(b), the produced NPs were well segregated and very porous. The present NPs exhibited irregular and angular nanostructure with high porous network, whereby proved that the aggregation of NPs was reduced by *C. esculenta* leaf extract. Almost a similar finding was reported by the authors of [42] that utilized an orange peel extract to use as a capping as well as reducing agent for synthesis of titanium oxide NPs. The EDX spectrum confirmed the chemical compositions and purity of CeO_2-NPs produced (Figure 4(c)). The strong cerium (Ce) peaks between 1.0 and 6 keV arise, according to the research. The presence of cerium and oxygen in synthesized NPs are shown by the spectrum peak. This was in accordance to the finding by Mary Isabella Sonali et al. [33] who synthesized CeO_2-NPs by using a bacterial strain. Another possible peak was contributed by carbon (C), potassium (K), phosphorus (P), sulfur (S), calcium (Ca), and chlorine (Cl) at a very low percentage (2% and below). The same finding was observed in the work reported by [39], in the synthesis of CeO_2-NPs by using *Elaeis guineensis* (oil palm) leaves, whereby the author reported the presence of C, P, and K in their NPs.

3.5. TEM Analysis. The morphological properties and average grain size of CeO_2-NPs made from *C. esculenta* leaf extract were examined by using transmission electron microscopy. TEM micrographs of produced CeO_2-NPs at scales of 10 nm shown in Figure 5(a). The TEM images revealed that the sample was completely invented of spherical, smooth, and far less agglomerated particles. Figure 5(b) shown a histogram obtained for the distribution of CeO_2-NPs at 10 nm size by using 50 particles. The average particle size was found to be 2.04 nm, which was found to be

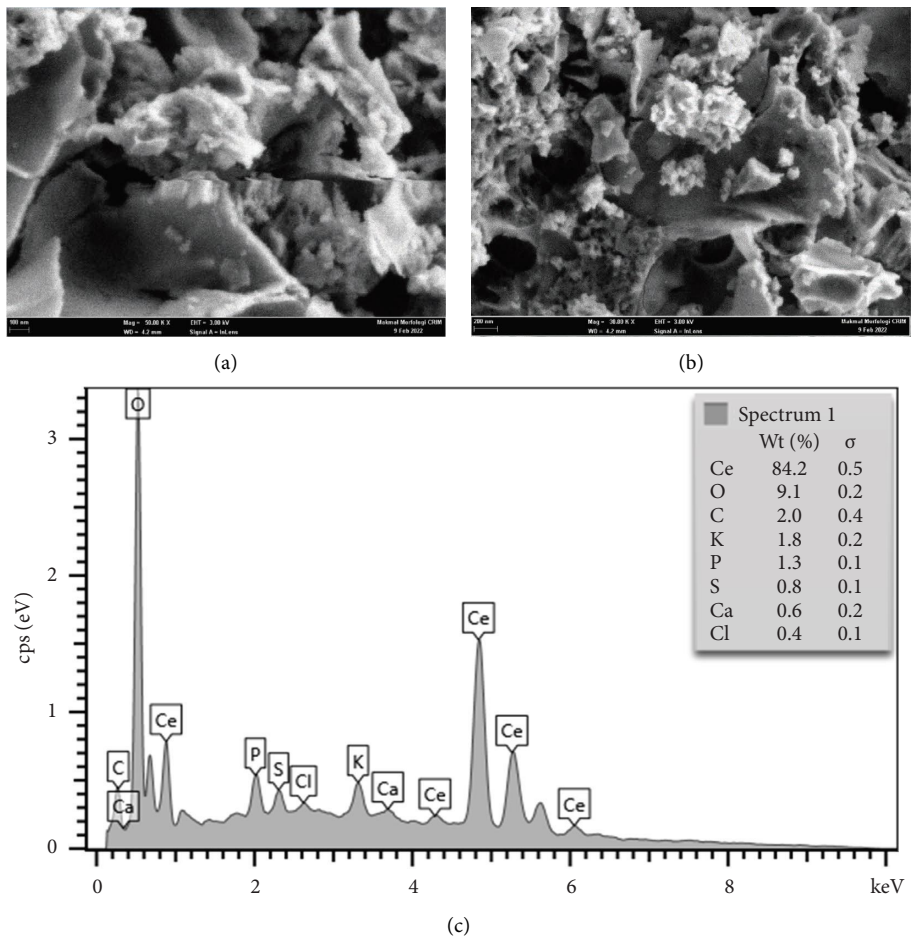

Figure 4: SEM images of CeO_2 nanoparticles at (a) 100 nm and (b) 200 nm and (c) EDX spectrum.

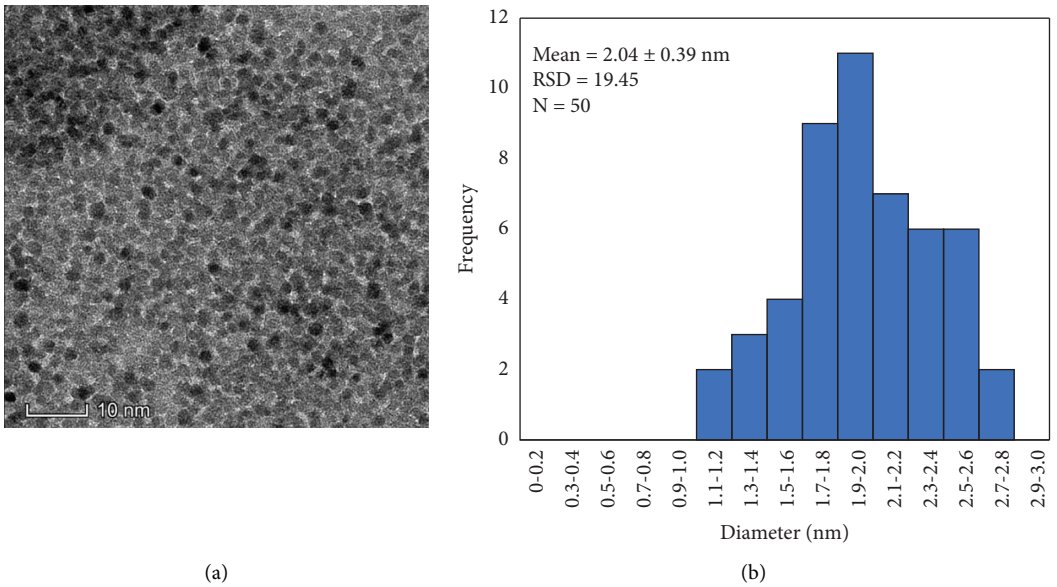

Figure 5: TEM image (a) and (b) histogram obtained for CeO_2-NPs at 10 nm.

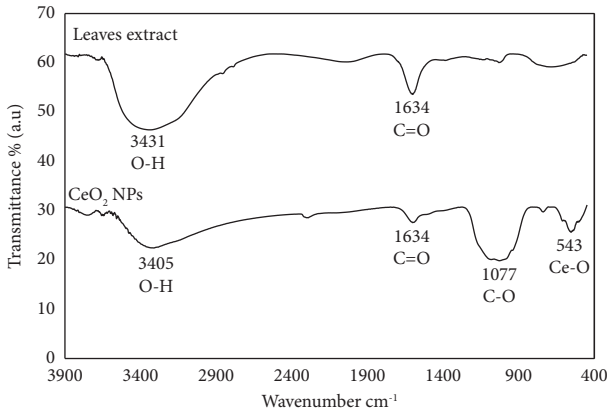

Figure 6: FTIR spectrum of leaves extract and CeO_2 nanoparticles.

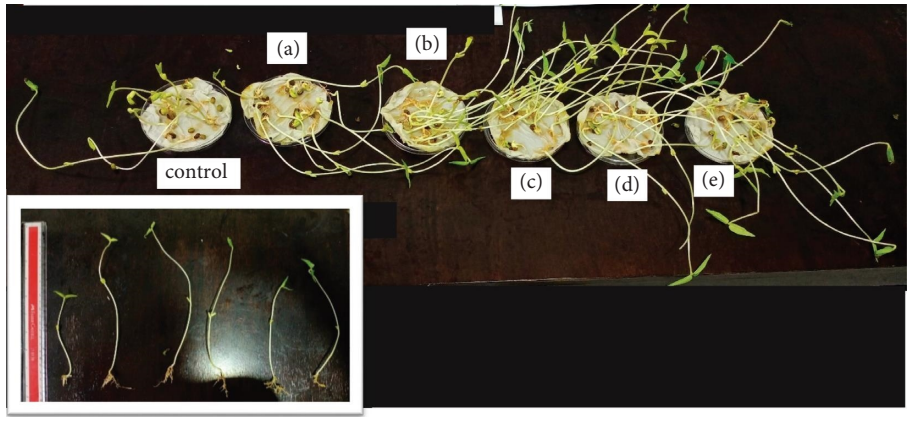

Figure 7: Seedling growths of *Vigna radiata* seeds of control: (a) 0.5 mg/mL, (b) 1.0 mg/mL, (c) 1.5 mg/mL, (d) 2.0 mg/mL, and (e) 2.5 mg/mL.

Table 1: Impact of CeO_2-NPs on root and shoot length per plant grown under screenhouse conditions.

Concentrations (mg/ml)	Root lengths (cm)	Shoot lengths (cm)
0	1.24 ± 1.25^{a}	8.01 ± 1.44^{ab}
0.5	1.91 ± 1.56	10.9 ± 1.45
1.0	2.81 ± 1.81^{abc}	16.5 ± 1.41^{a}
1.5	1.82 ± 1.37^{c}	10.8 ± 1.48
2.0	1.35 ± 1.52^{b}	12.0 ± 1.60
2.5	1.93 ± 1.73	14.6 ± 1.49^{b}

The values were given as mean ± SE (standard error) of triplicate samples with 15 seeds each. Similar letters within column indicate significant difference at $P < 0.05$ by using Tukey's test.

consistent with Scherrer's formula, based on XRD pattern. The tiny size was likely owing to the superior capping agent found in *C. esculenta* leaf extract, which prevented over-agglomeration during the nucleation and ageing stages of CeO_2-NP production. Koyyati et al. [43] reported a similar finding in the creation of zinc oxide NPs by using radish (Raphanus sativus) leaves, whereby very small NPs of 2 nm were formed, indicating the plant extract are rich in phytochemical elements to operate as a capping agent to control the size of NPs.

3.6. FTIR Analysis. FTIR spectra were obtained to identify the functional groups of CeO_2-NPs produced from *C. esculenta* leaf extract (Figure 6). Results of FTIR study in leaves extract exhibited transmittance peaks located at about 3431 cm^{-1}, indicating the presence of O-H functional group. The significant functional group was observed at 1634 cm^{-1} (C=O) due to the presence of carboxylic acids and esters from phytochemical constituent from the plant extract. The presence of peaks at around 3400 cm^{-1} and 1600 cm^{-1} were well agreed by the authors of [40] who reported the synthesis

of CeO_2-NPs in five different extracts of *Coriandrum sativum* (Coriander), *Phoenix dactylifera* (Ajwa dates), *Camellia sinensis* (green tea), *Ocimum tenuiflorum* (Black tulsi), and Hibiscus flower. In addition, spectrum of CeO_2-NPs revealed the peaks observed at 448 cm^{-1} confirmed the formation of CeO_2-NPs caused by the bond of Ce-O. This finding was in agreement to (Vasudevan) [44], whereby CeO_2-NPs were successfully synthesized by using *Justicia Adathoda* leaves extract, indicated by the presence of peak at 500 cm^{-1}. Likely, similar observation was reported by Parvathy et al. [45] who used *Artabotrys hexapetalus* leaf extract to prepare CeO_2-NPs. Significant peaks at 3405 cm^{-1}, 1634 cm^{-1}, and 1077 cm^{-1} were found similar with the work reported by Butt et al. [46] by using petals of Cinnamon-like bark *Cassia glauca* as a capping agent in the synthesis of CeO_2-NPs.

3.7. Effect on CeO_2-NPs Suspensions on Seedling Growth. In recent years, nanofertilizer of CeO_2-NPs had been reported to enhance the growth of plants. For example, Abdulhameed et al. [16] produced CeO_2-NPs by using laser ablation which yielded a very significant contribution to the growth of cabbage. Similarly, Mary Isabella Sonali et al. studied CeO_2-NPs of a germination of fenugreek seeds [33], whereby only 75 ppm of nanosized CeO_2-NPs in nanocomposite, the NPs were able to increase the shoot and root length of fenugreek plant. The present works were subsequently found to be in accordance to the previous findings as presented in Figure 7 and Table 1. Results showed that there was a significant difference ($P < 0.05$) between concentration of NPs with root and shoot length of mung bean seedling growth. The increasing concentration of CeO_2-NPs resulted in a notable increased length of root and shoot growth. Seed treated with CeO_2-NPs was found with increased value of root and shoot length as compared to control (untreated seeds). After 7 days of seedling growth, the optimum growth response for root and shoot in mung bean seedling was recorded at 1 mg/mL concentration with 2.81 ± 1.81 and 16.5 ± 1.41, respectively. This similar phenomenon also was observed in a study by Jayarambabu et al. [47] by using a similar plant seed, however with different concentrations and types of NPs. However, it was found that greater CeO_2-NP concentrations resulted in a considerable reduction in root and shoot length. The hazardous amount of NPs could explain the decline in root and shoot growth at higher doses. This was strong evidence that mung bean seedlings responded to NPs in a limited range, above which hazardous levels were obtained, resulting in growth reduction. Results were aligned with the previous study reported by López-Moreno et al. [48, 49] which showed an increasing root and shoot length in Zea mays and Glycine mays L. seedling treated by CeO_2-NP, respectively.

4. Conclusion

In this work, CeO_2-NPs were successfully prepared by using plant waste from *Colocasia esculenta*. Based on the characterization via XRD, the crystal size of CeO_2-NPs, calculated by using Debye–Scherrer equation, was found to be 2.94 nm and was found consistent with analysis from TEM. The CeO_2-NPs were found promising in mung bean (*Vigna radiata*) seed germination. In future, cytotoxicity study will be examined after the germination to study the toxic effects towards an optimized concentration.

Data Availability

The experimental data used to support the findings of the study are included in the paper.

Conflicts of Interest

The authors declare that they have no conflicts of interest.

Acknowledgments

The authors would like to thank Universiti Teknologi MARA Shah Alam and Universiti Teknologi MARA Negeri Sembilan Branch for the assistance and facilities provided throughout the research. The authors acknowledge the Centre for Research and Instrumentation Management (CRIM) for the analytical services given. The chemicals and facilities were provided by Universiti Teknologi MARA Shah Alam and Universiti Teknologi MARA Negeri Sembilan Branch.

References

[1] M. Auffan, J. Rose, J.-Y. Bottero, G. V. Lowry, J.-P. Jolivet, and M. R. Wiesner, "Towards a definition of inorganic nanoparticles from an environmental, health and safety perspective," *Nature Nanotechnology*, vol. 4, no. 10, pp. 634–641, 2009.

[2] M. Lal, P. Sharma, and C. Ram, "Calcination temperature effect on titanium oxide (TiO2) nanoparticles synthesis," *Optik*, vol. 241, pp. 1–14, 2021.

[3] S. Kanimozhi, R. Durga, M. Sabithasree et al., "Biogenic synthesis of silver nanoparticle using cissus quadrangularis extract and its in vitro study," *Journal of King Saud University Science*, vol. 34, no. 4, Article ID 101930, 2022.

[4] D. Sachan, A. Ramesh, and G. Das, "Green synthesis of silica nanoparticles from leaf biomass and its application to remove heavy metals from synthetic wastewater: a comparative analysis," *Environmental Nanotechnology, Monitoring & Management*, vol. 16, pp. 100467–100469, 2021.

[5] P. N. Kirdat, P. B. Dandge, R. M. Hagwane, A. S. Nikam, S. P. Mahadik, and S. T. Jirange, "Synthesis and characterization of ginger (z. officinale) extract mediated iron oxide nanoparticles and its antibacterial activity," *Materials Today: Proceedings*, vol. 43, pp. 2826–2831, 2021.

[6] K. R. Shubhashree, R. Reddy, A. K. Gangula et al., "Green synthesis of copper nanoparticles using aqueous extracts from Hyptis suaveolens (L.)," *Materials Chemistry and Physics*, vol. 280, no. 1–9, Article ID 125795, 2022.

[7] F. Asgharzadeh, A. Hashemzadeh, F. Rahmani et al., "Cerium oxide nanoparticles acts as a novel therapeutic agent for ulcerative colitis through anti-oxidative mechanism," *Life Sciences*, vol. 278, pp. 119500–119509, 2021.

[8] P. Maleki, F. Nemati, A. Gholoobi, A. Hashemzadeh, Z. Sabouri, and M. Darroudi, "Green facile synthesis of silver-

doped cerium oxide nanoparticles and investigation of their cytotoxicity and antibacterial activity," *Inorganic Chemistry Communications*, vol. 131, pp. 108762–108769, 2021.

[9] L. C. Dewberry, S. M. Niemiec, S. A. Hilton et al., "Cerium oxide nanoparticle conjugation to microRNA-146a mechanism of correction for impaired diabetic wound healing," *Nanomedicine: Nanotechnology, Biology and Medicine*, vol. 40, pp. 1–10, 2022.

[10] M. Sridharan, P. Kamaraj, J. Arockiaselvi, T. Pushpamalini, P. Vivekanand, and S. Hari Kumar, "Synthesis, characterization and evaluation of biosynthesized Cerium oxide nanoparticle for its anticancer activity on breast cancer cell (MCF 7)," *Materials Today: Proceedings*, vol. 36, pp. 914–919, 2021.

[11] V. D. C. Tinh, V. D. Thuc, and D. Kim, "Chemically sustainable fuel cells via layer-by-layer fabrication of sulfonated poly(arylene ether sulfone) membranes containing cerium oxide nanoparticles," *Journal of Membrane Science*, vol. 634, pp. 1–13, 2021.

[12] K. P. P. Bisquera, J. R. Salazar, E. S. Romero, L. Mar, A. Lopez, and J. J. Monserate, "Synthesis and characterization as zinc oxide nanoparticles as a source of zinc micronutrient in organic fertilizer," *International Journal of Agricultural Technology*, vol. 13, pp. 1695–1706, 2017.

[13] M. Arumugam, D. B. Manikandan, E. Dhandapani et al., "Green synthesis of zinc oxide nanoparticles (ZnO NPs) using Syzygium cumini: potential multifaceted applications on antioxidants, cytotoxic and as nanonutrient for the growth of Sesamum indicum," *Environmental Technology & Innovation*, vol. 23, pp. 1–16, 2021.

[14] A. Abbasifar, F. Shahrabadi, and B. ValizadehKaji, "Effects of green synthesized zinc and copper nano-fertilizers on the morphological and biochemical attributes of basil plant," *Journal of Plant Nutrition*, vol. 43, no. 8, pp. 1104–1118, 2020.

[15] A. Shebl, A. A. Hassan, D. M. Salama, M. E. Abd El-Aziz, and M. S. A. Abd Elwahed, "Green synthesis of nanofertilizers and their application as a foliar for cucurbita pepo L," *Journal of Nanomaterials*, vol. 2019, Article ID 3476347, 11 pages, 2019.

[16] M. F. Abdulhameed, A. A. Taha, and R. A. Ismail, "Improvement of cabbage growth and yield by nanofertilizers and nanoparticles," *Environmental Nanotechnology, Monitoring & Management*, vol. 15, pp. 100437-100438, 2021.

[17] S. Shinde, P. Paralikar, A. P. Ingle, and M. Rai, "Promotion of seed germination and seedling growth of Zea mays by magnesium hydroxide nanoparticles synthesized by the filtrate from Aspergillus Niger," *Arabian Journal of Chemistry*, vol. 13, no. 1, pp. 3172–3182, 2020.

[18] S. S. Mathew, N. E. Sunny, and V. Shanmugam, "Green synthesis of anatase titanium dioxide nanoparticles using Cuminum cyminum seed extract; effect on Mung bean (Vigna radiata) seed germination," *Inorganic Chemistry Communications*, vol. 126, pp. 108485–108487, 2021.

[19] J. Cyriac, K. Melethil, B. Thomas, M. Sreejit, and T. Varghese, "Synthesis of biogenic ZnO nanoparticles and its impact on seed germination and root growth of Oryza sativa L. and Vigna unguiculata L," *Materials Today Proceedings*, vol. 25, pp. 224–229, 2020.

[20] B. Gisela Manuela de França, J. Degenhardt, L. Alberto Zevallos Torres, and C. R. S. Valcineide Oliveira de Andrade Tanobe, "Green biosynthesis of single and bimetallic nanoparticles of iron and manganese using bacterial auxin complex to act as plant bio-fertilizer," *Biocatalysis and Agricultural Biotechnology*, vol. 30, pp. 1–9, 2020.

[21] D. Kim, R. G. Saratale, S. Shinde, A. Syed, F. Ameen, and G. Ghodake, "Green synthesis of silver nanoparticles using Laminaria japonica extract: characterization and seedling growth assessment," *Journal of Cleaner Production*, vol. 172, pp. 2910–2918, 2018.

[22] P. Chandrasekaran, G. Viruthagiri, and N. Srinivasan, "The effect of various capping agents on the surface modifications of sol-gel synthesised ZnO nanoparticles," *Journal of Alloys and Compounds*, vol. 540, pp. 89–93, 2012.

[23] R. Sathyamoorthy, K. Mageshwari, S. S. Mali, S. Priyadharshini, and P. S. Patil, "Effect of organic capping agent on the photocatalytic activity of MgO nanoflakes obtained by thermal decomposition route," *Ceramics International*, vol. 39, no. 1, pp. 323–330, 2013.

[24] G. Absalan, M. Akhond, H. Ershadifar, and M. A. Rezaei, "Two-approach study for preparing stable colloidal gold nanoparticles in organic solvents by using 1-dodecyl-3-methylimidazolium bromide as an efficient capping and phase transfer agent," *Colloids and Surfaces A: Physicochemical and Engineering Aspects*, vol. 486, pp. 192–202, 2015.

[25] K. K. Nishad, M. A. Manthrammel, M. Shkir, S. AlFaify, and R. K. Pandey, "Effect of organic capping on defect induced ferromagnetism in ZnO nanoparticles," *Physica B: Condensed Matter*, vol. 624, pp. 1–6, 2022.

[26] S. Singh, I. C. Maurya, A. Tiwari, P. Srivastava, and L. Bahadur, "Green synthesis of TiO2 nanoparticles using Citrus limon juice extract as a bio-capping agent for enhanced performance of dye-sensitized solar cells," *Surfaces and Interfaces*, vol. 28, pp. 101652–101659, 2022.

[27] F. Ferreres, R. F. Gonçalves, A. Gil-Izquierdo et al., "Further knowledge on the phenolic profile of Colocasia esculenta (L.) Shott," *Journal of Agricultural and Food Chemistry*, vol. 60, no. 28, pp. 7005–7015, 2012.

[28] I. Inamuddin and S. Kanchi, "One-pot biosynthesis of silver nanoparticle using Colocasia esculenta extract: colorimetric detection of melamine in biological samples," *Journal of Photochemistry and Photobiology A: Chemistry*, vol. 391, pp. 112310–112318, 2020.

[29] S. Alexandra, N. Jamora, M. Smale, and M. E. Ghanem, "The tale of taro leaf blight: a global effort to safeguard the genetic diversity of taro in the Pacific," *Food Security*, vol. 12, no. 5, pp. 1005–1016, 2020.

[30] S. Awan, K. Shahzadi, S. Javad, A. Tariq, A. Ahmad, and S. Ilyas, "A preliminary study of influence of zinc oxide nanoparticles on growth parameters of *Brassica oleracea* var italic," *Journal of the Saudi Society of Agricultural Sciences*, vol. 20, no. 1, pp. 18–24, 2021.

[31] S. Utara, S. Hunpratub, S. Pinitsoontorn, and S. Phokha, "Characterization and magnetic performance of pure CeO2 nanoparticles via an ozonolysis reaction," *Results in Physics*, vol. 30, Article ID 104890, pp. 1–10, 2021.

[32] J. Calvache-Muñoz, F. A. Prado, and J. E. Rodríguez-Páez, "Cerium oxide nanoparticles: synthesis, characterization and tentative mechanism of particle formation," *Colloids and Surfaces A: Physicochemical and Engineering Aspects*, vol. 529, pp. 146–159, 2017.

[33] J. Mary Isabella Sonali, R. Kavitha, P. S. Kumar et al., "Application of a novel nanocomposite containing micro-nutrient solubilizing bacterial strains and CeO2 nanocomposite as biofertilizer," *Chemosphere*, vol. 286, pp. 131800–131809, 2022.

[34] D. Parimi, V. Sundararajan, O. Sadak, S. Gunasekaran, S. S. Mohideen, and A. Sundaramurthy, "Synthesis of positively and negatively charged CeO2 nanoparticles: investigation of the role of surface charge on growth and

development of *Drosophila melanogaster*," *ACS Omega*, vol. 4, no. 1, pp. 104–113, 2019.

[35] A. Arumugam, C. Karthikeyan, A. S. Haja Hameed, K. Gopinath, S. Gowri, and V. Karthika, "Synthesis of cerium oxide nanoparticles using Gloriosa superba L. leaf extract and their structural, optical and antibacterial properties," *Materials Science and Engineering: C*, vol. 49, pp. 408–415, 2015.

[36] A. Krishnamoorthy, P. Sakthivel, I. Devadoss, and V. M. Illayaraja Muthaiyaa, "Structural, morphological and photoluminescence characteristics of Cd0.9-xZn0.1S quantum dots: effect of Fe2+ ion," *Optik*, vol. 205, pp. 164220–164229, 2020.

[37] G. Eka Putri, Y. Rilda, S. Syukri, A. Labanni, and S. Arief, "Highly antimicrobial activity of cerium oxide nanoparticles synthesized using Moringa oleifera leaf extract by a rapid green precipitation method," *Journal of Materials Research and Technology*, vol. 15, pp. 2355–2364, 2021.

[38] G. Tailor, B. L. Yadav, J. Chaudhary, M. Joshi, and C. Suvalka, "Green synthesis of silver nanoparticles using Ocimum canum and their anti-bacterial activity," *Biochemistry and Biophysics Reports*, vol. 24, pp. 1–5, 2020.

[39] T. Ahmad, J. Iqbal, M. A. Bustam et al., "Phytosynthesis of cerium oxide nanoparticles and investigation of their photocatalytic potential for degradation of phenol under visible light," *Journal of Molecular Structure*, vol. 1217, pp. 128292–128299, 2020.

[40] A. Iqbal, A. S. Ahmed, N. Ahmad et al., "Biogenic synthesis of CeO2 nanoparticles and its potential application as an efficient photocatalyst for the degradation of toxic amido black dye," *Environmental Nanotechnology, Monitoring & Management*, vol. 16, pp. 100505–100516, 2021.

[41] S. Aseyd Nezhad, A. Es-haghi, and M. H. Tabrizi, "Green synthesis of cerium oxide nanoparticle using *Origanum majorana* L. leaf extract, its characterization and biological activities," *Applied Organometallic Chemistry*, vol. 34, no. 2, pp. 1–10, 2019.

[42] A. Mobeen Amanulla and R. Sundaram, "Green synthesis of TiO2 nanoparticles using orange peel extract for antibacterial, cytotoxicity and humidity sensor applications," *Materials Today: Proceedings*, vol. 8, pp. 323–331, 2019.

[43] R. Koyyati, P. C. Latha, R. Sandupatla, V. Laxman, and R. Merugu, "Evaluation of anti-bacterial and rice seed germination potential of green and chemically synthesized ZnO nanoparticles," *Materials Today: Proceedings*, vol. 44, pp. 2611–2616, 2021.

[44] P. Vasudevan, "Biogenic synthesis of Cerium oxide nanoparticles using Justicia Adathoda leaves extract: size-strain study by X-ray peak profile analysis and luminescence characteristics," *Journal of Molecular Structure*, vol. 1272, pp. 1–10, 2023.

[45] S. Parvathy, G. Manjula, R. Balachandar, and R. Subbaiya, "Green synthesis and characterization of cerium oxide nanoparticles from Artabotrys hexapetalus leaf extract and its antibacterial and anticancer properties," *Materials Letters*, vol. 314, pp. 131811–131814, 2022.

[46] A. Butt, J. S. Ali, A. Sajjad, S. Naz, and M. Zia, "Biogenic synthesis of cerium oxide nanoparticles using petals of Cassia glauca and evaluation of antimicrobial, enzyme inhibition, antioxidant, and nanozyme activities," *Biochemical Systematics and Ecology*, vol. 104, pp. 104462–104469, 2022.

[47] N. Jayarambabu, B. S. Kumari, K. V. Rao, and Y. T. Prabhu, "Germination and growth characteristics of mungbean seeds (Vigna radiata L.) affected by synthesized zinc oxide nanoparticles," *International Journal of Current Engineering and Technology*, vol. 4, no. 5, pp. 3411–3416, 2014.

[48] M. L. López-Moreno, G. De La Rosa, J. A. Hernández-Viezcas et al., "Evidence of the differential biotransformation and genotoxicity of ZnO and CeO2 nanoparticles on soybean (Glycine max) plants," *Environmental Science and Technology*, vol. 44, no. 19, pp. 7315–7320, 2010.

[49] M. L. López-Moreno, G. de la Rosa, J. A. Hernández-Viezcas, J. R. Peralta-Videa, and J. L. Gardea-Torresdey, "X-Ray absorption spectroscopy (XAS) corroboration of the uptake and storage of CeO_2 nanoparticles and assessment of their differential toxicity in four edible plant species," *Journal of Agricultural and Food Chemistry*, vol. 58, no. 6, pp. 3689–3693, 2010.